Published in Journal of Materials Chemistry 9, issue 5, 1085-1090, 1999
which should be used for any reference to this work

First ferrocene-containing low molar mass organosiloxane liquid-crystalline materials

Harry J. Coles,[a]* Sebastien Meyer,[a] Petra Lehmann,[a] Robert Deschenaux[b] and Isabelle Jauslin[b]

[a]*Southampton Liquid Crystal Institute, Department of Physics and Astronomy, University of Southampton, Southampton, UK SO17 1BJ. E-mail: hjc@lc.phys.soton.ac.uk; http://www.slci.soton.ac.uk*
[b]*Institut de Chimie, Université de Neuchâtel, Av. de Bellevaux 51, 2000 Neuchâtel, Switzerland*

Two ferrocene-containing low molar mass organosiloxane liquid-crystalline materials have been synthesised and their phase-transition behaviour investigated. The ω-unsaturated ferrocene precursor was hydrosilylated by addition of pentamethyldisiloxane or heptamethyltrisiloxane in the presence of platinum divinyltetramethyldisiloxane complex. The ferrocene precursor presents smectic A and smectic C phases; the disiloxane compound exhibits a smectic C phase; the trisiloxane compound shows a smectic C phase and two higher order smectic phases. Tilt angle measurements were performed on samples oriented on polytetrafluoroethylene (PTFE) friction deposited layers since rubbed polyimide (PI) only gave very poor alignment. For the precursor the tilt angle was found to be very small, close to 2°, while for the two organosiloxane ferrocene compounds it was close to 28° and almost independent of temperature. These compounds exhibited ferroelectric electro-optic switching properties when doped with 1–2% w/w of chiral mesogens.

Introduction

There is a growing interest in metal-containing liquid-crystalline materials[1,2] that combine some of the properties of metals with those of mesogenic moieties since this could lead to processable materials with interesting anisotropic optical, electronic and magnetic properties. Owing to its unique redox characteristics, ferrocene is a valuable unit for building up switchable systems[3] and recently, electron transfer was used to generate mesomorphism in the ferrocene–ferrocenium redox system.[4]

Ferrocene-containing side-chain liquid-crystal polymers (SCLCPs) have been reported in the literature.[1,2,5] The SCLCPs offer several advantages over the low molar mass liquid crystals in that they have better mechanical characteristics, a broader mesomorphic range and a reduced or suppressed tendency to form crystalline phases. However, because of the rigidity of the polymer backbone, the SCLCPs are usually highly viscous and therefore have long switching response times.[6] The SCLCPs based on flexible polysiloxane backbones have shorter response times than those based on more rigid polymers such as the polymethacrylates. Furthermore, the polydispersity of the commercially available materials is a serious problem for the production of materials with reproducible characteristics.[6] Recently, several low molar mass liquid-crystalline organosiloxanes have been developed[6–9] that show fast electro-optic responses whilst retaining some of the ruggedness of the polymeric systems.[6] They display mainly smectic phases due to the micro-segregation of the mesogenic, paraffinic and siloxane moieties into distinct sublayers within the lamellar phase[7,8] and a resultant agglomeration of the siloxane units into a 'virtual' backbone.[9] The smectic layers, for fractionated monodisperse siloxane moieties, are particularly well defined and the isotropic to smectic phase transition is normally first order. For polydisperse siloxane groups the phase sequence may be altered and the materials tend to favour lower order smectic phases.[10] This is important in the present work since we will present the synthesis and thermal properties of the first ferrocene-containing low molar mass and monodisperse organosiloxane liquid-crystalline materials (structures **2** and **3**), which represent a novel family of metal-based anisotropic materials (see Synthesis and Fig. 1). We will present data for two homologues, containing 2 and 3 silicon atoms, in comparison with the ω-unsaturated ferrocene precursor. This will allow us to demonstrate that, despite its relatively small size compared to the bulky ferrocene mesogenic group, the siloxane moiety plays an important role in the phase stability, phase sequence, electro-optic properties and quality of the surface alignment.

Experimental

Synthesis

The ferrocene precursor **1** was synthesised as previously described.[2] 1,1,1,3,3-Pentamethyldisiloxane, 1,1,1,3,3,5,5-heptamethyltrisiloxane and the platinum catalyst (platinum–divinyltetramethyldisiloxane complex, 3–3.5% platinum concentration in vinyl terminated polydimethylsiloxane, neutral) were purchased from Fluorochem. Toluene was freed of thiophene according to standard procedures and then dried over sodium in the presence of benzophenone.

^{1}H and ^{13}C NMR spectra were recorded on a Bruker AC 300 spectrometer. Mass spectra were recorded on a Micromass Platform quadrupole mass analyser with an electrospray ion source.

Compounds **2** and **3** were synthesised following the procedure outlined in Fig. 1.

0.1 mmol of the precursor **1** and the platinum catalyst were dissolved in 1 ml of toluene under dry argon such that a Pt : alkene ratio in the range $1:10^4$–10^6 was obtained. The solution was stirred at 60 °C for one hour. 0.11 mmol of the hybrid functionalised siloxane was added. The reaction mixture was stirred at 90 to 100 °C for three days. Fresh catalyst was added every 24 h. On cooling, the solvent was removed under reduced pressure. The crude product was passed through a silica gel column (Merck, Si60, 40–63 μm) using dichloromethane as the eluent, and re-precipitated in methanol and hexane until no amount of precursor could be detected.

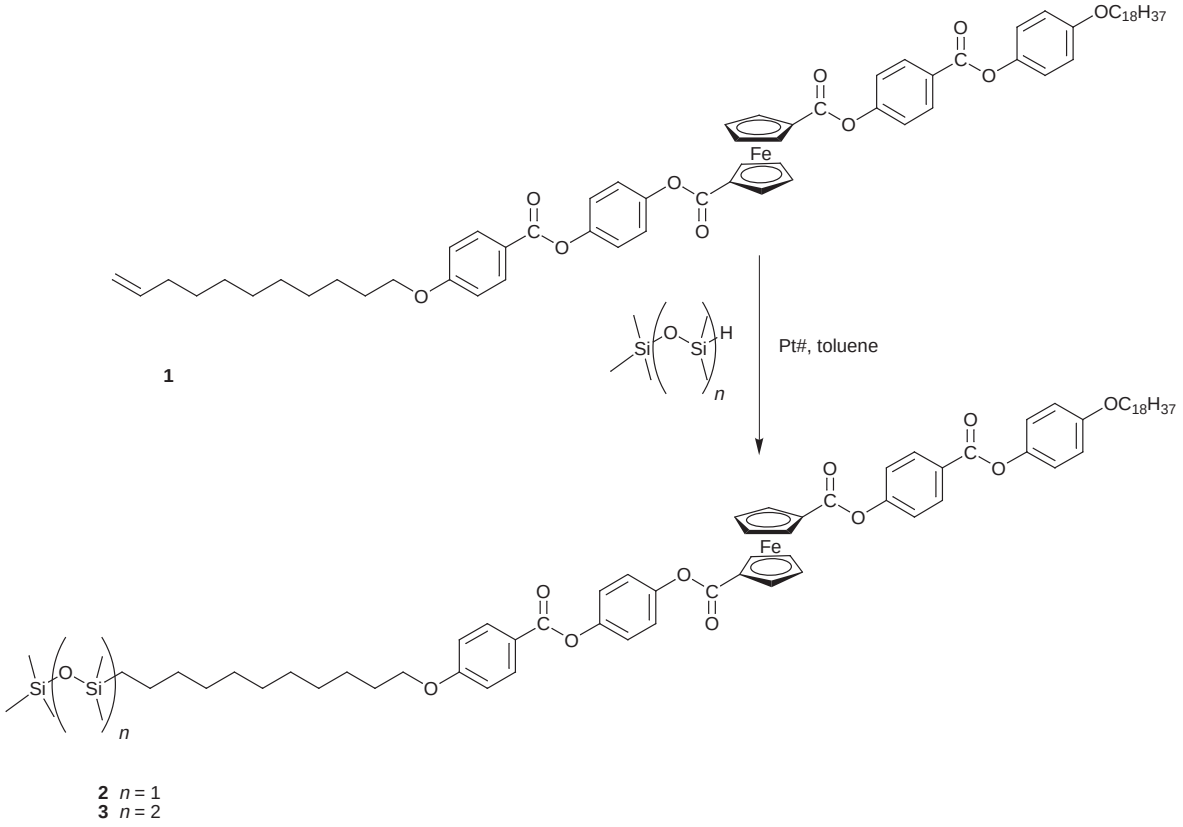

Fig. 1 Synthetic route to compounds **2** and **3**.

Freeze-drying from benzene gave the pure product in high yield.

1-[4-(4-(11-(1,1,1,3,3-Pentamethyldisiloxyl)undecyloxy)-benzoyloxy)phenyl]-1′-[4-(4-octadecyloxyphenyloxycarbonyl)-phenyl]ferrocenedicarboxylate (2). Yield: 89%; ^{1}H NMR (300 MHz, $CDCl_3$) δ: 0.0–0.2 (m, 15 H, Si-CH_3), 0.56 (m, 2 H, Si-CH_2), 0.90 (t, 3 H, CH_3). 1.2–1.9 (m, 50 H, CH_2), 3.97 (t, 2 H, CH_2-O), 4.05 (t, 2 H, CH_2-O), 4.64 (m, 4 H, Cp), 5.10 (m, 4 H, Cp), 6.95–7.40 (m, 12 H, aromatic), 8.11–8.26 (m, 4 H, aromatic); ^{13}C NMR (300 MHz, $CDCl_3$) δ: 0.23, 1.31, 1.82, 14.15, 18.30, 22.70, 26.00, 29.73, 31.94, 33.46, 114.27, 115.09, 121.35, 122.37, 127.10, 131.75, 132.30, 144.18, 147.96, 148.45, 154.79, 156.88, 163.59, 164.82, 168.82; ES MS m/z: 1269.5 $(M+NH_4)^+$, 1276.5 $(M+Na)^+$.

1-[4-(4-(11-(1,1,1,3,3,3,5,5-Heptamethyltrisiloxyl)-undecyloxy)benzoyloxy)phenyl]-1′-[4-(4-octadecyloxyphenyl-oxycarbonyl)phenyl]ferrocenedicarboxylate (3). Yield: 85%; ^{1}H NMR (300 MHz, $CDCl_3$) δ: 0.0–0.2 (m, 21 H, Si-CH_3), 0.57 (m, 2 H, Si-CH_2), 0.92 (t, 3 H, CH_3), 1.2–1.9 (m, 50 H, CH_2), 3.95 (t, 2 H, CH_2-O), 4.06 (t, 2 H, CH_2-O), 4.66 (m, 4 H, Cp), 5.11 (m, 4 H, Cp), 6.95–7.38 (m, 12 H, aromatic), 8.12–8.25 (m, 4 H, aromatic); ^{13}C NMR (300 MHz, $CDCl_3$) δ: 0.22, 1.29, 1.83, 14.14, 18.29, 22.71, 26.01, 29.72, 31.93, 33.47, 114.29, 115.08, 121.33, 122.39, 127.11, 131.76, 132.31, 144.19, 147.98, 148.47, 154.80, 156.90, 163.58, 164.81, 168.80; ES MS m/z: 1342.5 $(M+NH_4)^+$, 1347.3 $(M+Na)^+$, 1363.5 $(M+K)^+$.

Physical characterisation

The mesomorphic properties of the compounds synthesised (**1–3**) were studied by thermal optical microscopy and differential scanning calorimetry (DSC). The DSC measurements were carried out on a Perkin-Elmer DSC7 instrument on samples weighing between 2 and 4 mg and at scanning rates of 5 °C min^{-1} (**1** and **2**) and 2 °C min^{-1} (**3**) (Fig. 2). Phase characterisation by polarised light microscopy was carried out using an Olympus BH-2 microscope equipped with a TMS91 Linkam hot stage stable to 0.1 °C over a temperature range from −196 °C to 600 °C. The enthalpies and temperatures of the phase transitions are reported in Table 1. Preliminary powder X-ray diffraction was carried out using an apparatus previously described,[7] to confirm the basic phase structure.

Results and discussion

The precursor (compound **1**) gives smectic A and smectic C phases over temperature ranges of 12.5 °C and 12 °C respectively, with a clearing temperature at 146.5 °C. Attaching the pentamethyldisiloxane or heptamethyltrisiloxane units, for compounds **2** and **3** respectively, suppresses the smectic A

Table 1 Enthalpies and temperatures of phase transitions

Compound	Phase transitions, T/°C (ΔH/J g^{-1})					
1	K–S_C	122 (39.1)	S_C–S_A	134[a]	S_A–I 146.5 (10.9)	
2	K–S_C	125.3 (18.6)	S_C–I	142.8 (8.4)		
3	K–S_2	122 (16.8)	S_2–S_1	123.6[a] (0.3[b])	S_1–S_C 124.5[a] (2.5[b])	S_C–I 135.6 (6.7)

[a]Determined by polarized optical microscopy. [b]Determined from second DSC cooling run.

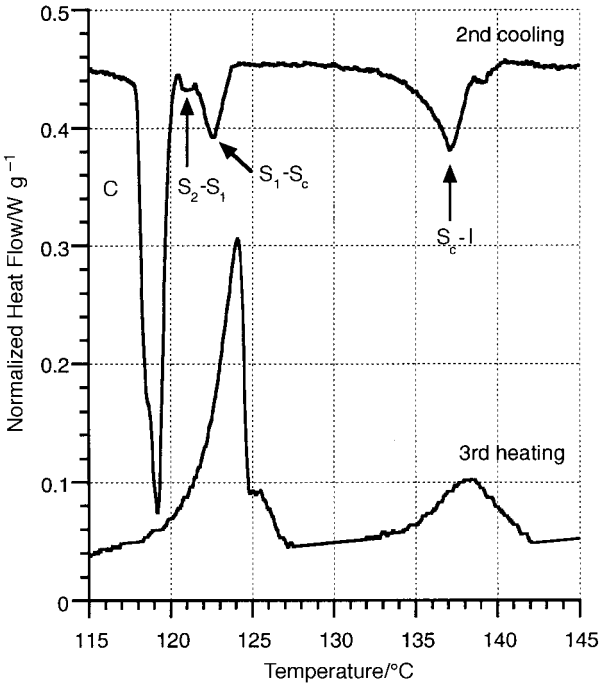

Fig. 2 DSC Thermograms (second cooling and third heating) of compound **3**.

phase and both materials exhibit a direct isotropic to smectic C phase on cooling (Fig. 2). The clearing temperature decreased systemically, by a few degrees, with increasing siloxane content. For compound **2** the smectic C phase range is broadened to 17.5 °C and this was the only mesophase observed. However while compound **2** shows no paramorphotic textures, the DSC thermograms of compound **3** (with the longer siloxane chain) revealed the existence of two higher order smectic modifications (denoted 1 and 2) below the smectic C phase which is itself 11.1 °C wide. Of these two phase transitions only the smectic C→smectic 1 transition is unambiguously observed by thermal microscopy. This transition is marked by fluctuations of the *schlieren* brushes moving wave-like across the preparation. Compared to the *schlieren* texture displayed by the smectic C phase (Fig. 3a) the texture in the S_1 phase (Fig. 3b) appears to be 'frozen', with shadowed areas bordered by optical discontinuities. Comparing the observed textures with the available literature,[11] the corresponding phase could be assigned as the hexatic tilted smectic F or I. As these phases only differ in the tilt direction relative to the local hexagonal lattice, their textures are similar (*c.f.* Plates 85 and 86 and page 131 in ref. 11). Unless the two phases occur in sequence, which is not the case here, it is almost impossible to differentiate the phases (I and F) by optical microscopy alone. On further cooling the fans develop a striated texture, while the *schlieren* brushes start to disappear giving way to a shadowed mosaic texture (Fig. 3c). However, assigning these observed changes to the smectic 1→smectic 2 transition is not obvious as this texture does not seem to be thermodynamically very stable. Crystallisation takes place almost instantly. This is marked by the formation of bands across the focal-conic fans and the development of uniform domains consisting of overlapping platelets (Fig. 3d) and these are reminiscent of the texture displayed by the crystal E phase. To unambiguously define the smectic 1 and 2 phases we would need to carry out detailed X-ray analysis on aligned samples.[12] Miscibility studies with known smectic I and F materials are not an obvious experimental technique to use with the present materials since there are currently no known chemically compatible organosiloxane ferrocenes available that exhibit such phases.

We were not able to achieve a satisfactory alignment of the specimens on conventional rubbed polyimide (PI). Instead, the materials were aligned on friction deposited polytetrafluoroethylene (PTFE) using a technique developed by Wittmann and Smith.[13] Using the friction deposition apparatus described by Hanmer[14] and under optimal experimental conditions (temperature of 300 °C, pressure of 10^6 Pa and deposition rate of 0.25 mm s^{-1})[15] a very thin, around 20 to 30 nm thick, quasi-monocrystalline film with the PTFE chains aligned in the direction of friction (called the alignment direction hereafter), can be deposited on a hard counterface such as a glass slide. A wide range of crystalline and liquid crystalline materials have been successfully aligned on friction deposited PTFE layers.[13–18] Fig. 4 allows a comparison between the quality of alignment obtained with commercial rubbed PI (Fig. 4a) and friction deposited PTFE layers (Fig. 4b). Sample thicknesses are 10 μm. While only small mono-oriented domains could be grown on PI, large uniformly aligned films could be made on PTFE layers (notice the difference in scales in Fig. 4). As far as we are aware this is the first time that such good alignment has been demonstrated for ferrocene based liquid crystals.

The optical tilt angle θ (*i.e.* the angle between the director and the layer normal, *c.f.* Fig. 7) and the angle α between the PTFE alignment direction and the layer normal were measured using a method, described by Dierking *et al.*,[19] developed for smectic C* phases. To induce a smectic C* phase in our materials we prepared mixtures of the three compounds with a compatible (*i.e.* miscible) chiral dopant added in very low concentration (*i.e.* 1–2% w/w). We assume that such a low concentration will not affect the value of the optical tilt angle. For compound **1** we used SCE2 (Merck, UK) as the chiral additive, whilst for compounds **2** and **3** we used the chloro-substituted ferroelectric organosiloxanes, with 2 or 3 silicon atoms respectively, described elsewhere.[20] Besides providing a method for measuring the optical tilt angle the observed switching demonstrates that these organosiloxane grafted ferrocene materials are capable of exhibiting ferroelectric properties (Fig. 5). Cells made of PTFE covered ITO glass were filled with each mixture and we measured the light transmitted through the microscope with crossed polarisers when a square wave voltage is applied to the cell. With a field of 3 V μm^{-1} we found that this tilt angle was invariant with increasing field. The intensity of the transmitted light in the positive (δ_{pos}) and negative (δ_{neg}) switched states was recorded and plotted as a function of the rotation angle φ of the sample. $\varphi = 0$ was defined when the PTFE alignment direction was parallel to one of the crossed polarisers. The two intensity curves can be fitted by[20] the following equations:

$$I_{pos} = \sin^2(2(\varphi + \delta_{pos})) \text{ and } I_{neg} = \sin^2(2(\varphi - \delta_{neg}))$$

The optical tilt angle θ is then given by

$$\theta = \frac{\delta_{pos} + \delta_{neg}}{2}$$

At the position of the cross-over of the intensity curves, the two states appear the same and the corresponding value of φ is the angle α between the PTFE alignment direction and the layer normal. The values of the optical tilt angles are in agreement with those indicated by the preliminary X-ray measurements.[21] The layer spacing of the precursor (compound **1**) in the smectic A and C phases is $\approx$60.2 Å whilst in compounds **2** and **3** it is 54.8 Å and 55.6 Å, respectively. These latter values are independent of temperature, except very close to the clearing temperature.

The temperature dependences of θ and α are shown in Fig. 6(a) and (b) respectively. For compound **1**, the precursor, the optical tilt angle is very small, *i.e.* close to 2°, while α decreases slightly from 30° to 24° on reaching the smectic A

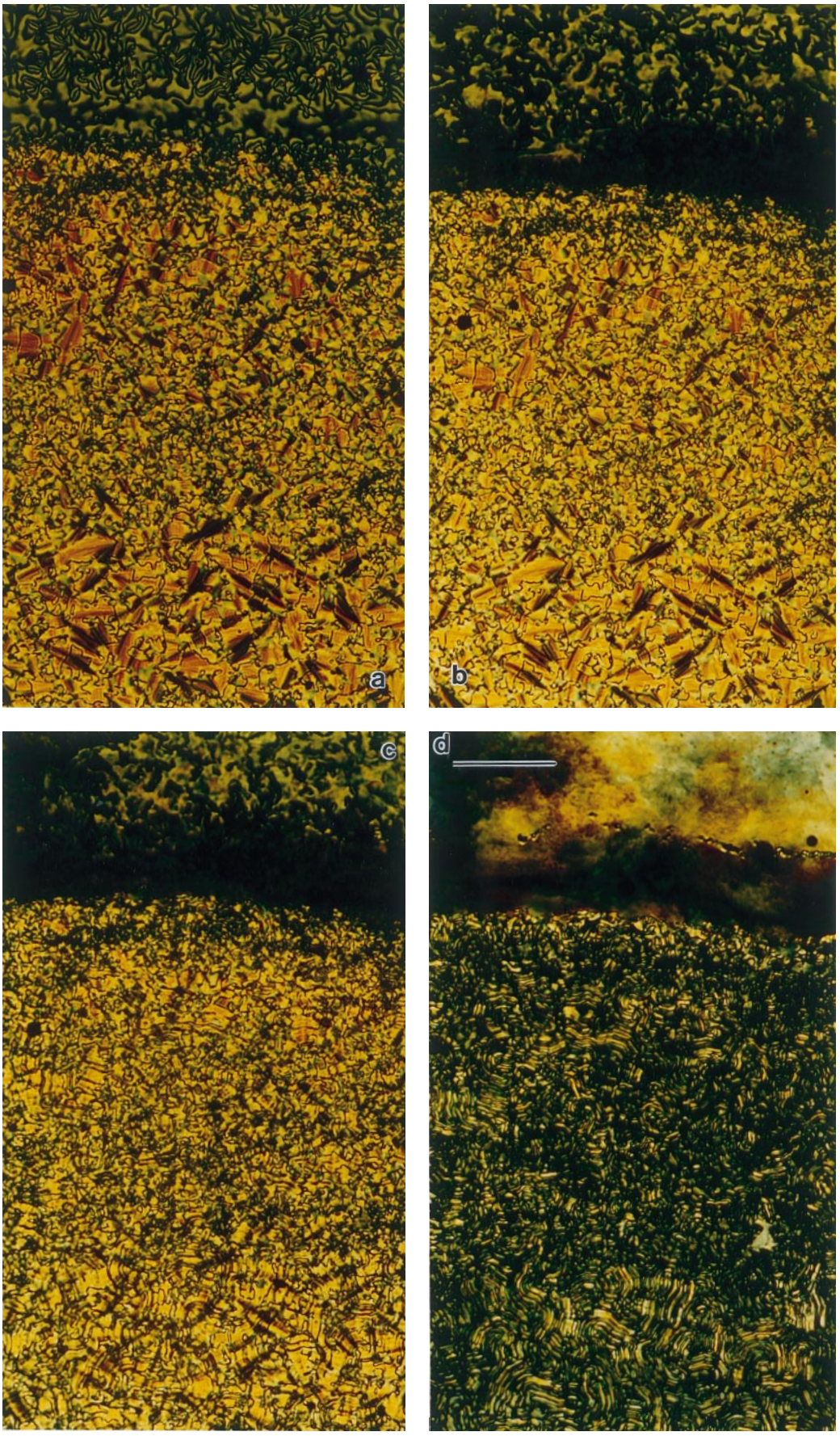

Fig. 3 Optical textures given on cooling of compound **3** using untreated glass substrates to promote both *schlieren* and focal-conic textures. Observation is between crossed polarisers. a) 127 °C. b) 124 °C. c) 123.4 °C. d) 120.4 °C. Scale bar corresponds to 100 μm.

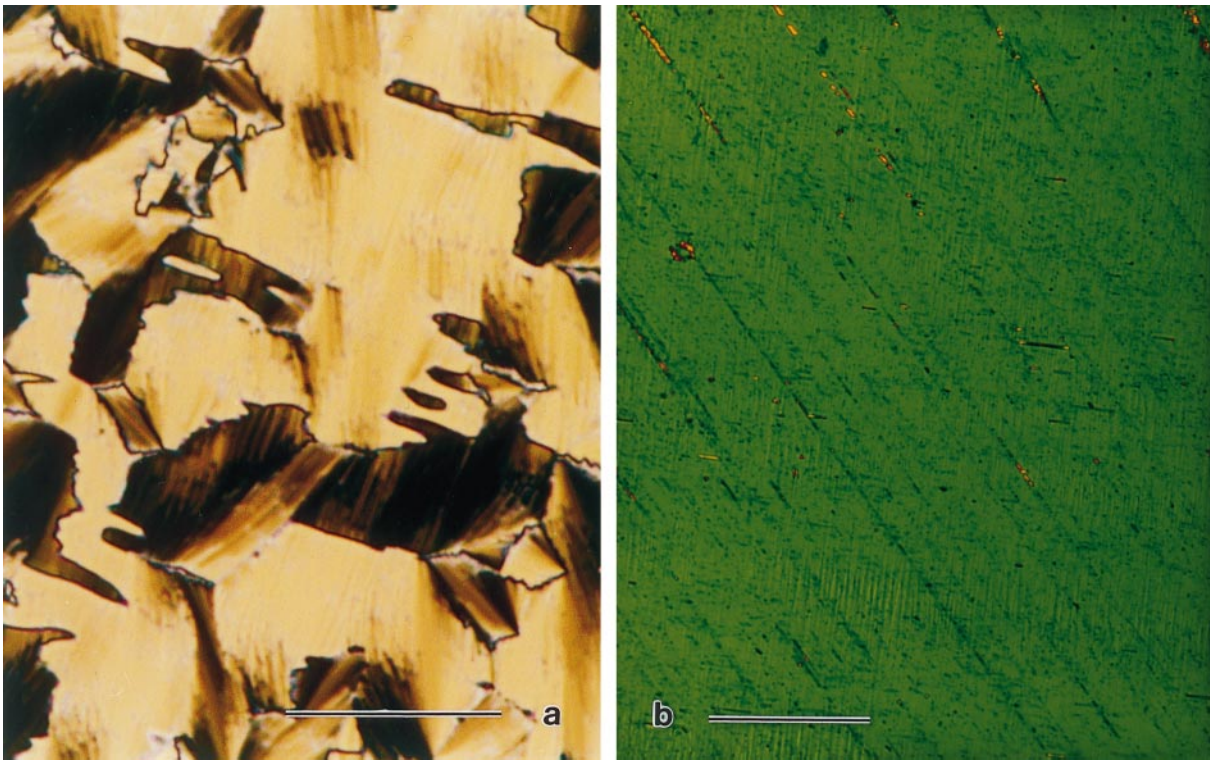

Fig. 4 Microphotography between crossed polarisers of compound **1** aligned on different substrates: a) rubbed polyimide, b) friction deposited PTFE. Scale bars correspond to 100 μm.

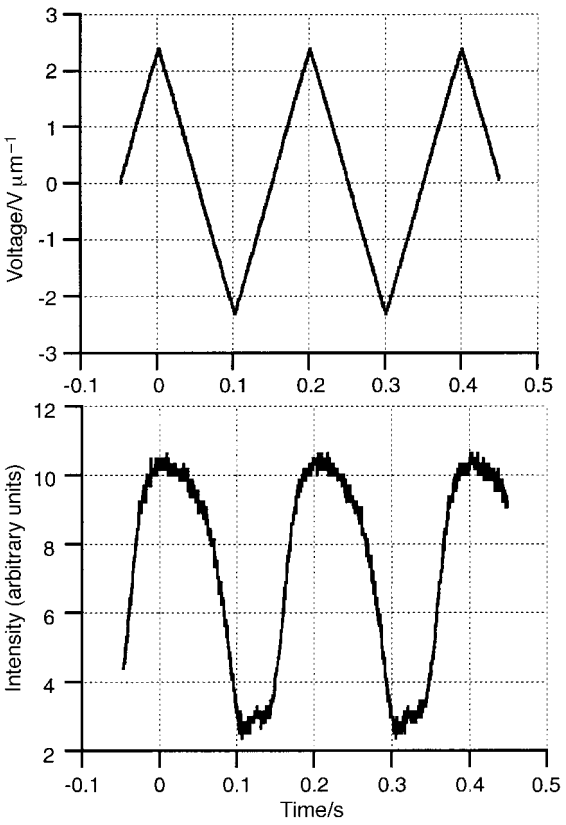

Fig. 5 Ferroelectric optical switch of compound **3** doped with the chiral additive. The upper trace shows the applied electric field whilst the lower shows the latched ferroelectric switching.

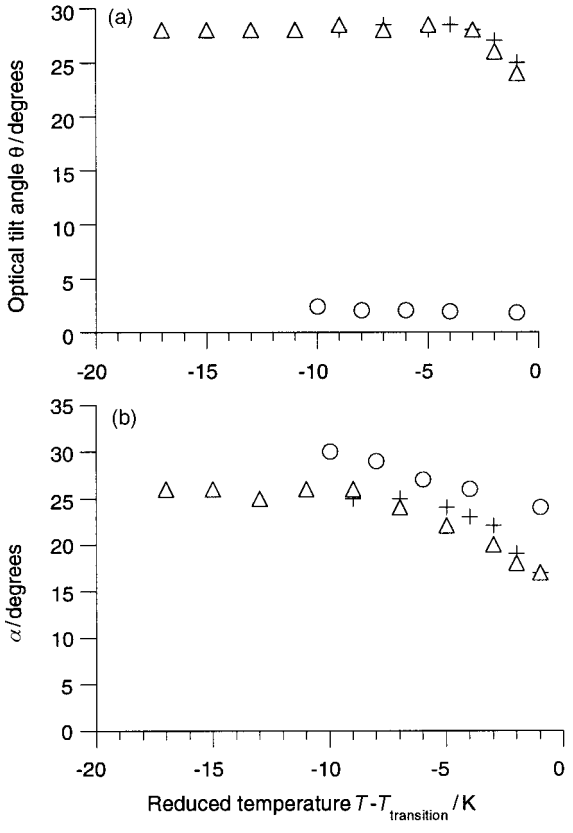

Fig. 6 (a) Temperature dependence of the optical tilt angle, ○: compound **1**, +: compound **2**, △: compound **3**. (b) Temperature dependence of the angle α between the PTFE alignment direction and the layer normal, ○: compound **1**, +: compound **2**, △: compound **3**.

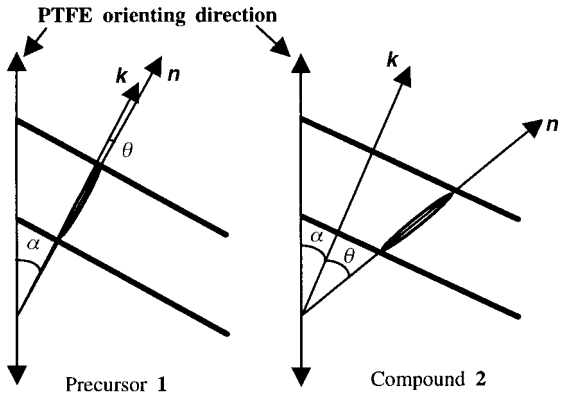

Fig. 7 Relative orientation of the layers (thick lines), director ***n***, layer normal ***k***, and PTFE orienting direction for the precursor **1** and compound **2**. The fine lines indicate the directions of ***n*** and ***k*** in each case. Typical values (*c.f.* Fig. 6) of θ and α are 2° and 26° for **1** and 28° and 24° for **2** respectively (data at $T - T_{\text{transition}} \approx -5°$).

phase. The introduction of a siloxane moiety increases dramatically the value of the tilt angles. For compounds **2** and **3**, the optical tilt angles are close to 28° (equivalent to a ferroelectric cone angle of 56°) over a wide temperature range while α decreases from 24° to 17° with increasing temperature. The difference between the optical tilt angles of the siloxane compounds and the precursor is extremely high, *i.e.* 26°, and this is much higher than in a similar comparison for other low molar mass organosiloxane liquid-crystalline materials,[22] where the increase due to hydrosilylation was typically 3–4°. Since the values of the angle α (*i.e.* between the layer normal and the PTFE alignment direction), for the precursor and the siloxane compounds, only differ by around 6° the increased difference in the optical tilt angles is not due to a tilting of the layer but is caused by a tilt of the molecules within the layers. Fig. 7 shows the relative orientations of the layers and the molecules with respect to the PTFE alignment direction. Thus addition of the siloxane units has an extremely marked effect on the orientation of the mesogens in the smectic layer. This is all the more remarkable when the size ratio of the ferrocene mesogenic and siloxane moieties is taken into account.

Conclusion

We have successfully synthesised the first ferrocene containing low molar mass organosiloxane liquid-crystalline materials. By using PTFE friction-deposited films as alignment substrates we have managed to obtain large planar oriented domains in 10 μm thick cells. DSC measurements and optical microscopy observations have shown that the grafting of a siloxane moiety leads to a broadening of the smectic C phase as well as suppression of the smectic A phase observed in the precursor compound. This grafting leads to a marked increase of the tilt angle for the organosiloxane based compounds in comparison with the precursor. Additionally, the longer heptamethyltrisiloxane unit induces two, as yet unidentified, higher order smectic phases. The tilt angles are independent of the temperature apart from within a 3° wide pretransitional region at the smectic C to isotropic phase transition. Thus the organosiloxane based ferrocenes show liquid crystalline properties remarkably different from those of the vinyl precursor. Further addition of chiral dopants has allowed ferroelectric properties to be demonstrated, for the first time, in these compounds. We are currently researching into the origins of this ferroelectric behaviour and its implications for the other electromagnetic properties of these new organometallic materials.

Acknowledgements

HJC thanks the EPSRC for a research grant GR/K/70908 and Merck UK Ltd for studentship support for PL. We thank Dr Carboni for useful discussions and Dr Guillon (IPCMS) Strasbourg for providing the X-ray facilities.

References

1 (*a*) R. Deschenaux and J. W. Goodby, in *Ferrocenes*, ed. A. Togni and T. Hayashi, VCH, Weinheim, 1995, ch. 9; (*b*) P. Zanello, in *Ferrocenes*, ed. A. Togni and T. Hayashi, VCH, Weinheim, 1995, ch. 7.
2 (*a*) R. Deschenaux, I. Kosztics, U. Scholten, D. Guillon and M. Ibn-Elhaj, *J. Mater. Chem.*, 1994, **4**, 1351; (*b*) R. Deschenaux, I. Jauslin, U. Scholten, F. Turpin, D. Guillon and B. Heinrich, *Macromolecules*, 1998, **31**, 5647.
3 J. C. Medina, I. Gay, Z. Chen, L. Echegoyen and G. W. Gokel, *J. Am. Chem. Soc.*, 1991, **113**, 365.
4 R. Deschenaux, M. Schweissguth and A.-M. Levelut, *Chem. Commun.*, 1996, 1275.
5 R. Deschenaux, V. Izvolenski, F. Turpin, D. Guillon and B. Heinrich, *Chem. Commun.*, 1996, 439.
6 J. Newton, H. J. Coles, P. Hodge and J. Hannington, *J. Mater. Chem.*, 1994, **4**, 869.
7 M. Ibn-Elhaj, H. J. Coles, D. Guillon and A. Skoulios, *J. Phys. II (France)*, 1993, **3**, 1807.
8 E. Corsellis, D. Guillon, P. Kloess and H. J. Coles, *Liq. Cryst.*, 1997, **23**, 235.
9 H. J. Coles, H. Owen, J. Newton and P. Hodge, *Liq. Cryst.*, 1993, **15**, 739.
10 M. Redmond, H. J. Coles, E. Wischerhoff and R. Zentel, *Ferroelectrics*, 1993, **148**, 323.
11 G. W. Gray and J. W. Goodby, *Smectic Liquid Crystals—Textures and Structures*, Leonard-Hill, London, 1984.
12 R. Date, G. R. Luckhurst, M. Shuman and J. M. Seddon, *J. Phys. II (France)*, 1995, **5**, 587.
13 J.-C. Wittmann and P. Smith, *Nature*, 1991, **352**, 414.
14 J. Hanmer, PhD Thesis, University of Manchester, 1995.
15 S. Meyer, Doctorate es Sciences Thesis, University Louis Pasteur Strasbourg, 1995.
16 J.-C. Wittmann, S. Meyer, P. Damman, M. Dosiere and H.-W. Schmidt, *Polymer*, 1998, **39**, 3545.
17 M. Suzuki, A. Ferenez, S. Iida, V. Enkelmann and G. Wegner, *Adv. Mater.*, 1993, **5**, 359.
18 G. Lester, J. Hanmer and H. Coles, *Mol. Cryst. Liq. Cryst.*, 1995, **262**, 149.
19 I. Dierking, F. Gießelmann, J. Schacht and P. Zugenmaier, *Liq. Cryst.*, 1995, **19**, 179.
20 W. K. Robinson, C. Carboni, P. Kloess, S. P. Perkins and H. J. Coles, *Liq. Cryst.*, 1998, **25**, 301.
21 H. Allouchi, unpublished preliminary X-ray data taken at IPCMS, Strasbourg.
22 P. Kloess, Ph.D. Thesis, University of Southampton, 1997.